

PAPER • OPEN ACCESS

Liquid hydrogen storage and transfer-control system for integrated zero emission aviation (IZEA)

To cite this article: IZEA Collaboration *et al* 2024 *IOP Conf. Ser.: Mater. Sci. Eng.* **1302** 012024

View the [article online](#) for updates and enhancements.

You may also like

- [Influence of surface roughness on multidiffusive mixed convective nanofluid flow](#)

P M Patil, A Shashikant, P S Hiremath *et al.*

- [Research on Leakage and Diffusion characteristics of Liquid Hydrogen Based on Gaussian Diffusion Model](#)

Bangkai Shi, Yanwei Chen, Yang Hu *et al.*

- [Numerical Simulation of Liquid Hydrogen Spilling in the Confined Cabin with Air Supplying and Vent](#)

Z Y Shu, WQ Liang, G Lei *et al.*

UNITED THROUGH SCIENCE & TECHNOLOGY

 **The Electrochemical Society**
Advancing solid state & electrochemical science & technology

**248th
ECS Meeting**
Chicago, IL
October 12-16, 2025
Hilton Chicago

**Science +
Technology +
YOU!**

Abstract submission
deadline extended:
April 11, 2025

SUBMIT NOW

Liquid hydrogen storage and transfer-control system for integrated zero emission aviation (IZEA)

(IZEA Collaboration) P S Viridi ^{1,2}, W Guo ^{1, 2, *}, L Cattafesta ³, P Cheetham ^{1,4}, L Cooley ^{1,2,5}, J Gladin ^{6,7}, J He ^{8,9}, D M Ionel ^{8,9}, C Kim ⁴, H Li ^{1,4}, J Ordonez ^{1,4}, S Pamidi ^{1,4} and J Zheng ¹⁰

¹FAMU-FSU College of Engineering, Florida State University, Tallahassee, USA

²National High Magnetic Field Laboratory, Tallahassee, USA

³Illinois Institute of Technology, Chicago, USA

⁴Center for Advance Power Systems, Tallahassee, USA

⁵Applied Superconductivity Center, National High Magnetic Field Laboratory, Tallahassee, USA

⁶Georgia Institute of Technology, Atlanta, USA

⁷ Aerospace Systems Design Laboratory, Atlanta, USA

⁸ University of Kentucky, Lexington, USA

⁹ Power and Energy Institute of Kentucky, Lexington, USA

¹⁰ University at Buffalo, Buffalo, USA

Email: wguo@magnet.fsu.edu

Abstract. The growth in the aviation sector has highlighted the need to decrease carbon emissions, a significant factor in climate change. Hydrogen is a potential alternative clean fuel due to its high energy density. As a collaborative effort in developing integrated zero emission aviation (IZEA, a NASA ULI), we present the design concept for a liquid hydrogen storage system for short-range aircraft with a gravimetric index greater than 0.6. Our design leverages the cryogenic cooling power of liquid hydrogen to support the temperature and heat loads of various power system components, such as the high-temperature superconducting (HTS) generator, HTS motor, DC power distribution cable network, and power electronic converters. By controlling the pressure in the storage tank, we demonstrate that it is feasible to deliver the desired mass flow rate of hydrogen while effectively cooling the power system components using practical heat exchangers. Also, since heat exchangers are an integral part of our hydrogen storage and flow system, their design also impacts the overall system storage density. The entire system is designed considering the space and weight factors of an aircraft. This work represents a significant advancement towards developing the complete IZEA thermal management system for a given airplane and flight profile.

1. Introduction

IZEA (Integrated Zero Emissions Aviation) is a NASA ULI (University Leadership Initiative) which aims to develop a hybrid aircraft that uses liquid hydrogen as the aviation fuel. The global aviation market is growing, and the effects of rising emissions are a serious concern. This leads us to a search for an alternative fuel. Hydrogen is a clean fuel and has 2.8 times higher gravimetric energy density in comparison to the presently used aviation fuel, kerosene [1]. However, a known challenge is its low density. Hydrogen in its gas phase has a density of 0.08 kg/m³ at ambient temperature and pressure.



This low density can be increased by increasing the pressure or lowering the temperature, but for aviation purposes liquid hydrogen LH₂ appears to be the only feasible solution of storage. Hydrogen in its liquid form at 20.3 K and one atmospheric pressure has a density of 70.8 kg/m³. Even then, this requires four times the volume [1] as compared to the conventional jet fuel for the same energy amount. This brings in the requirement of the development of a model hybrid aircraft and an effective LH₂ fuel storage solution.

The proposed IZEA model aircraft is equipped with a hybrid hydrogen-electric propulsion architecture. The electricity is generated via a combination of hydrogen turboelectric generator(s) and fuel cells. Fuel cells operate at 350 K while the hydrogen is stored at 20.3 K in the storage tank. Our approach aims to utilize the cooling power of liquid hydrogen to cool down the power components in the power architecture and maintain them at the required operating temperatures. This requires the hydrogen stored in the tank to flow via a system of heat exchangers before it is utilized for electric power generation in a high temperature superconducting (HTS) generator or a fuel cell.

In this paper, we present the design of a liquid hydrogen tank along with the LH₂ fuel mass flow rate control system that can meet the power requirements based on a specific flight power profile.

2. Tank Design

A blended wing body aircraft provides more volume especially in the outer and rear fuselage parts as compared to the conventional aircraft [1]. IZEA presents a conceptual model of a LH₂-based blended wing body aircraft that carries more than 100 passengers. The baseline aircraft geometry is shown in Figure 1(a). It highlights the space layout for the LH₂ storage tank. The spatial constraint of the layout is shown in the adjacent 2D CAD Figure 1(b).

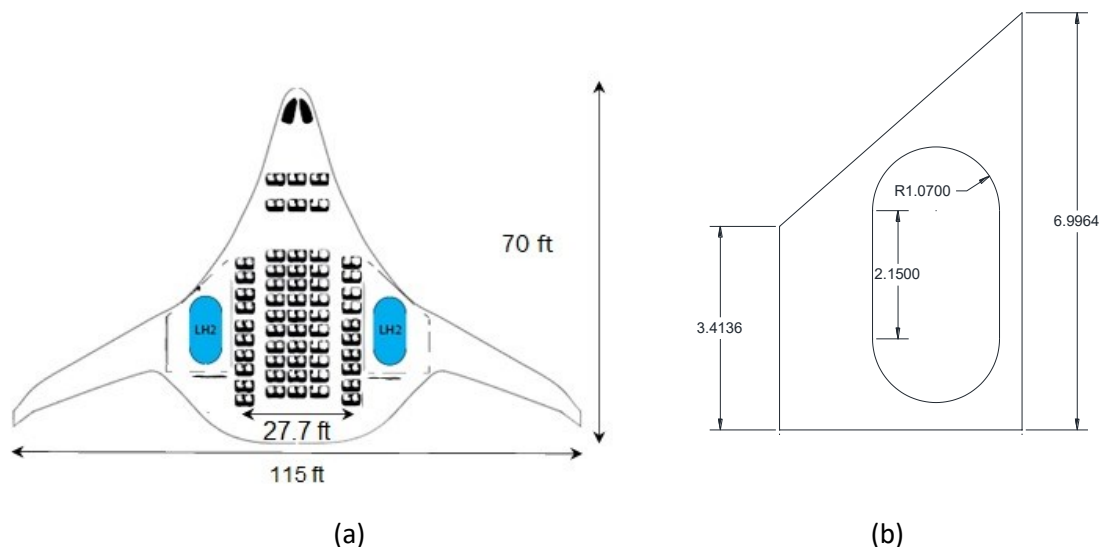


Figure 1. (a) Model aircraft's baseline geometry. **(b)** The space for liquid hydrogen tank storage in the left section of the aircraft. An optimal configuration of the liquid hydrogen storage tank is shown placed inside the space available.

A conventional narrow body aircraft flight mission profile is included in Figure 2 which shows the required power P_{req} versus time t for a given flight path [2]. The maximum power, which is 38 MW, occurs during the aircraft climbing stage.

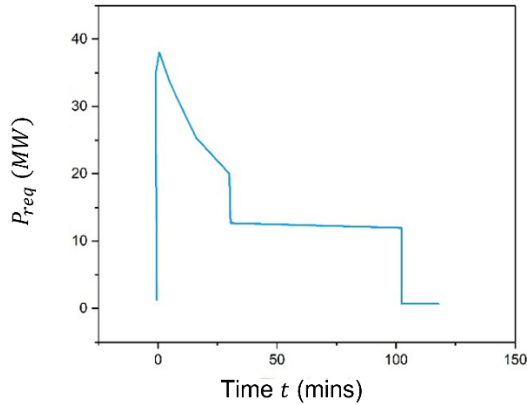


Figure 2. Flight Required Power Profile for narrow body aircraft.

2.1. Required Hydrogen Mass

IZEA embraces a flexible hybrid power generation concept, where LH₂ fuel is converted to energy by gas turbine combustion coupled with electric generators (i.e., turboelectric) and fuel cells. The hydrogen combustion releases 120 MJ/kg of energy [1]. Hydrogen is consumed in fuel cells to produce electric power. This conversion efficiency is around 50% [1], which translates to a chemical power P_{chem} profile as shown in Figure 3 (a). From the required chemical power profile, we obtain the required hydrogen mass flow rate \dot{m}_{req} as a function of time in Figure 3 (b).

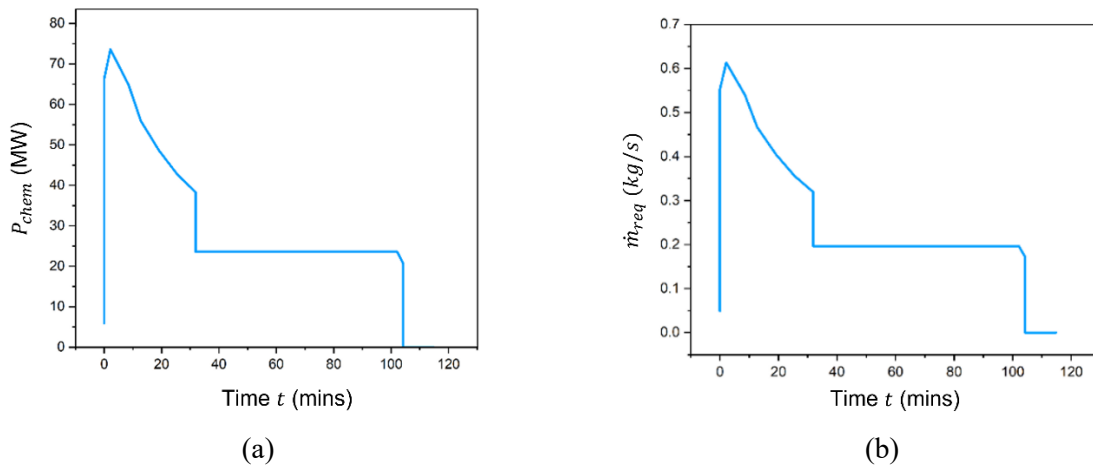


Figure 3. (a) The required chemical power as a function of flight time; and (b) The required mass flow rate as a function of flight time for the narrow body aircraft under consideration.

Integrating the mass flow rate over the flight time results in the total required hydrogen mass of 1750 kg, which needs to be carried in the aircraft to execute the flight mission profile.

Following the aircraft geometry outlined in Figure 1, this total required hydrogen mass needs to be distributed in two storage tanks, each placed symmetrically on the right and left side of the airplane. Therefore, each tank carries 875 kg of LH₂ which can be filled in a tank of 13 m³ volume.

2.2. Closed LH₂ Tank System

After the tank is filled with LH₂, we consider a flight waiting time τ_w before the flight takes off. During the flight waiting time, we would not like to waste any fuel by venting. This leads to a closed LH₂ tank system where the tank pressure P_{tank} rises due to the heat in-leak \dot{Q}_{leak} from the tank's surrounding environment to the LH₂ stored inside. The tank pressure P_{tank} is allowed to rise till it reaches the set tank vent pressure P_{vent} .

Also, as the pressure P rises, the liquid level y inside the closed tank increases as shown in Figure 4 (a). This happens because hydrogen vapor density increases with increasing pressure and the liquid density drops with increasing pressure as depicted in Figure 4 (b).

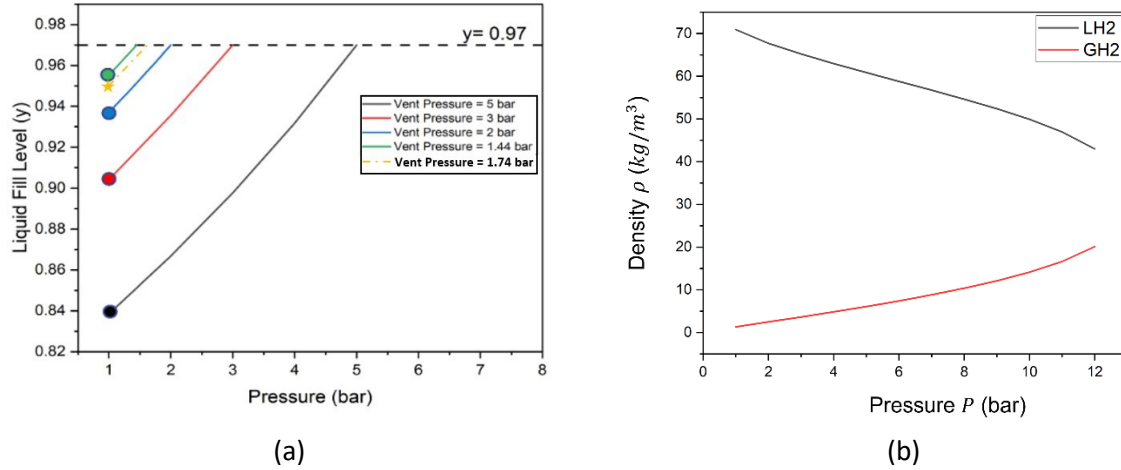


Figure 4 (a) . Rise in liquid level from an initial level to a set final level at 0.97 volume fraction for different vent pressures in a closed LH₂ tank. **(b)** Density variation with pressure for LH₂ and GH₂.

To avoid LH₂ spilling off the vent port, we set a maximum liquid level to 97% of the tank volume [1]. This limitation sets the initial fill level of the LH₂ at 1 bar. We would essentially want to fill our tank as much as possible utilizing the maximum possible volume available.

The tank vent pressure P_{vent} is an important parameter of the tank design in aviation because it determines the minimum tank wall thickness s_w , which affects the weight of the tank system. Winnefeld et. al (2018) proposed to keep a low vent pressure such as 1.448 bar to minimize tank weight which is in accordance with Brewer's suggestion [3]. Besides the consideration of tank weight, we also propose to control the flow rate of the LH₂ fuel by regulating the tank pressure. While the tank pressure P_{tank} is limited to the vent pressure P_{vent} , it should also be greater than fuel cell operating pressure. Under all such consideration we choose P_{vent} as 1.74 bar. As shown in Figure 4(a), this vent pressure corresponds to the initial fill level of 0.95 fraction of tank volume at 1 bar. This vent pressure P_{vent} is used to determine the tank wall thickness δ .

Heat leak rate \dot{Q}_{leak} is calculated using $(E_f - E_i)/\tau_w$, where $E_i = -1.2 MJ$ is the tank internal energy at time $t = 0$ when the tank is filled with LH₂ at 0.95 fraction of tank volume at pressure $P = 1 bar$ and temperature $T = 20 K$, $E_f = 16.3 MJ$ is the tank internal energy after flight waiting time $\tau_w = 80 mins$ during which the tank pressure reaches the vent pressure due to heat leak from the surroundings to the closed tank system. This heat leak rate $\dot{Q}_{leak} = 3.6 kW$ forms the basis of determining tank insulation thickness.

2.3. Storage Density

Storage Density χ is defined as $\chi = m_{H_2}/(m_{H_2} + m_{wall} + m_{ins})$, where m_{H_2} is LH₂ fuel mass, m_{wall} is tank wall mass and m_{ins} is tank insulation mass. For our application we need a tank geometrical configuration that provides the maximum storage density while complying with the space constraints inside the airplane. Here, we adopt the methodology developed by Winnefeld et al. (2018) where the different geometrical configurations are obtained for a fixed tank volume.

Tank geometry considered in our analysis is a shell with hemispherical cap as shown in Figure 5. The tank volume V can be calculated as $V = (4/3)\pi a c^2 + \pi a c l_s$, which is function of 3 variables (a , c , l_s). For a fixed volume, specifying any two variables automatically sets the third parameter. Here we

introduce two geometrical ratios to describe the geometry: $\phi = a/c$ and $\lambda = l_s/l_t$. In our analysis, ϕ is tuned from 0.5 to 1.5 and λ is tuned from 0.1 to 0.9.

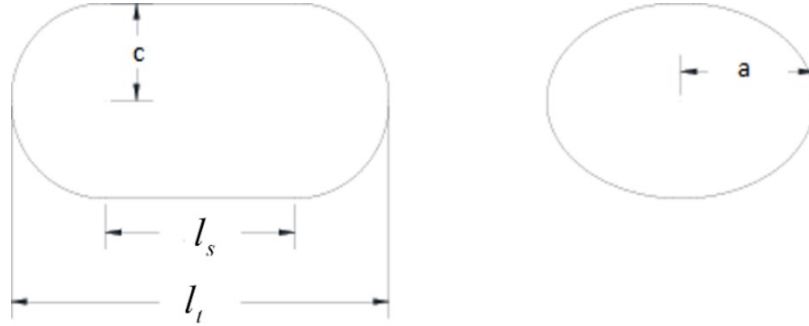


Figure 5. Description of the parameters generating different tank geometrical configurations of a constant tank volume ($V = 13 \text{ m}^3$).

For any given tank configuration, the tank wall thickness s_w is evaluated using equation (1) for $\phi = 1$ and equation (2) for $\phi \neq 1$ [1]:

$$s_w = \frac{p_{vent} D}{v \left(\frac{2K}{S} - p_{vent} \right)} + c_1 \quad (1)$$

$$\frac{K}{S} \geq p_{vent} \left[\frac{a+c}{2s_w} \left(1 + 2 \left(1 + 3.6 \frac{p_{vent}}{E_Y} \left(\frac{a+c}{2s_w} \right)^3 \right) \left(\frac{a-c}{a+c} \right) \right) + \frac{1}{2} \right] \quad (2)$$

where p_{vent} is the maximum tank internal pressure, K is the limited stress of the tank wall material, S is the safety factor which is taken as 4 following reference [4] and E_Y is the modulus of elasticity of the tank wall material. We take the tank wall material as Aluminium 2219 ([1],[5]-[7]).

Tank insulation thickness δ is calculated as:

$$\int_0^\delta \frac{\dot{Q}_{leak}}{A} dx = \int_{20K}^{T_o} k(T) dT \quad (3)$$

where T_o is the ambient temperature, A is the surface area and k is the thermal conductivity of the tank insulation material as a function of temperature. We take the tank insulation material as polyurethane foam [5],[8],[9]. Here, equation (3) only considers conduction through tank insulation since it is the major source of thermal resistance. After evaluating the tank wall thickness and tank insulation thickness for any given geometrical configuration, the tank wall mass and tank insulation mass can be calculated from which storage density can be determined for that geometrical configuration.

2.4. Result

The calculated storage density χ for various geometrical configurations is shown in Figure 6 (a) and 6 (b).

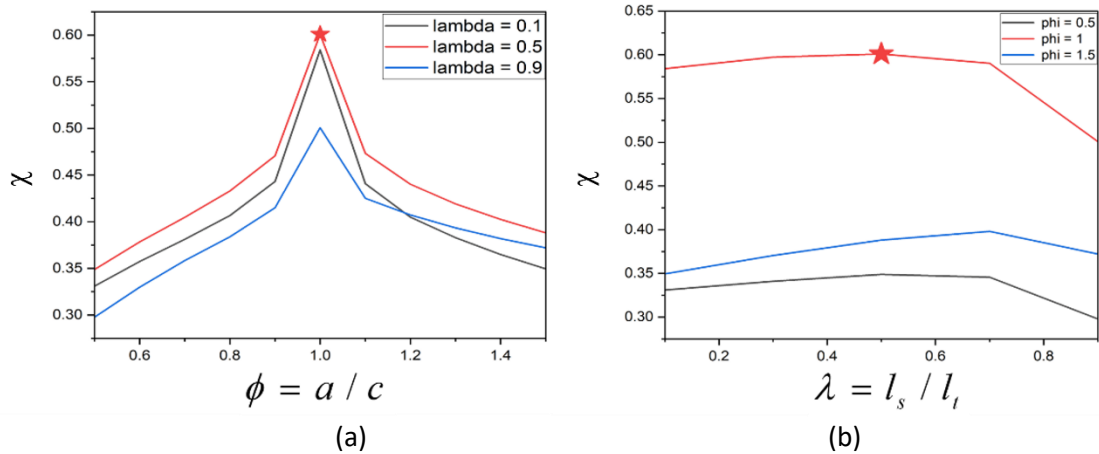


Figure 6 (a). Storage Density variation with Φ . (b) Storage Density variation with λ . Combination of Φ and λ at the maximum storage density value is the choice of tank configuration.

The storage density plots reveal maximum storage density for a cylindrical shell i.e., $\Phi = 1$. Highest storage density can be found for $\lambda = 0.5$. λ can be tuned around 0.5 without compromising much on the storage density in case space constraints restrict the tank placement. The tank with this optimal geometry is found to perfectly fit in the space specified in the model aircraft as shown in Figure 1.

For further accuracy of the tank insulation thickness and to ensure that the tank surface temperature (T_s) is above 273 K to avoid icing on the tank surface, the thermal resistance due to external surface convection was also considered on the optimal tank geometrical configuration. It was done by solving for the conduction through insulation using Equation (4a) and external convection using Equation (4b)

$$\int_0^\delta \frac{\dot{Q}_{leak}}{A} dx = \int_{20}^{T_s} k(T) dT \quad (4a)$$

$$\dot{Q}_{leak} = \frac{Nu_D k_{air}}{D} A (T_o - T_s) \quad (4b)$$

where the Nusselt Number and Rayleigh Number correlations for natural convection on a horizontally placed cylindrical tank were used for this calculation [10].

The optimal tank parameters derived through this analysis are listed in Table 1.

Table 1. Tank specifications and features

Description	Value
LH ₂ mass	875 kg
LH ₂ volume	13 m ³
Tank wall thickness	5.69 mm
Tank Wall Mass	463 kg
Ins. Thickness	5.3 cm
Tank Insulation Mass	54.3 kg

3. LH₂ Mass Flow Rate Control

Liquid Hydrogen fuel stored in two tanks inside the aircraft must flow at the desired mass flow rate to the fuel cell/ combustion engine. We propose to control this fuel mass flow rate by tuning the pressure inside the tank. This could avoid potential issues such as cavitation, heating etc. with cryo-fans [11].

The tuning range of tank pressure P_{tank} is within the maximum value of $P_{vent} = 1.74 \text{ bar}$ and minimum value of optimal fuel cell operating pressure, which is 1.3 bar [12].

This tank pressure can be controlled by two mechanisms: 1. controlled boiling and 2. venting. A hot fluid flowing inside a pipe immersed in the LH₂ tank is conceptualized as a controlled boiling mechanism as shown in Figure 7. Heat is transferred from this pipe to liquid hydrogen causing boil off, which increases the pressure inside the tank. Venting of GH₂ takes place through a vent port situated on the top of the tank. The pressure inside the tank is actively monitored by a pressure transducer [13] mounted on the tank whose feedback and the aircraft power requirement actuate the controlled boiling and venting mechanisms.

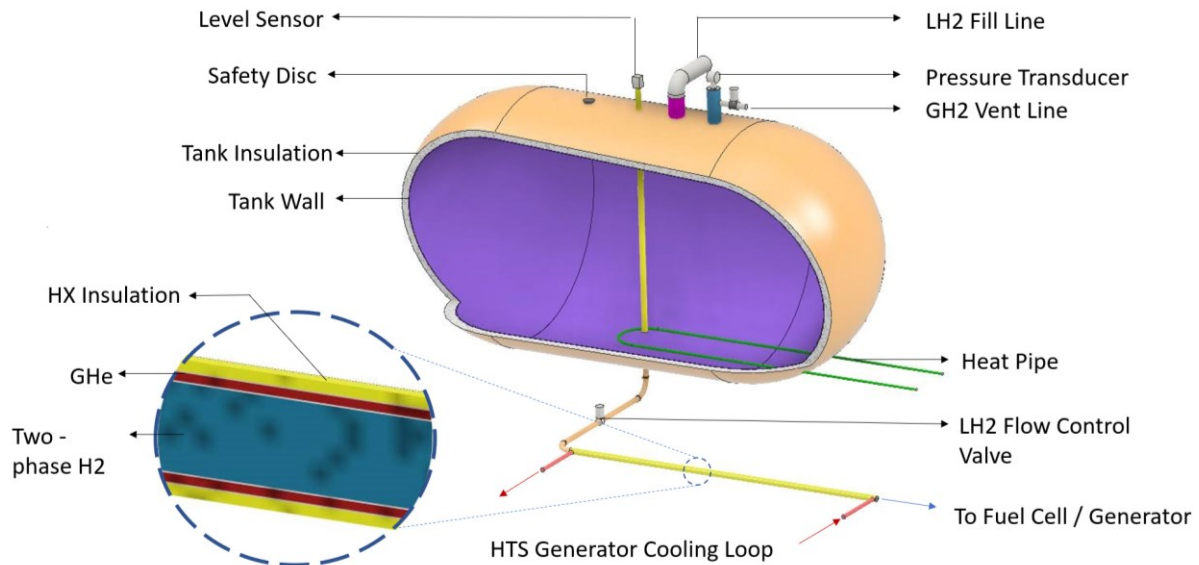


Figure 7. LH₂ Tank Schematic shows the cut-section view of the storage tank. The LH₂ fuel output line passes through a set of heat exchangers of which the first heat exchanger (pipe-in-pipe counter flow heat exchanger) which cools the HTS generator is shown.

From the storage tank, LH₂ must flow through a set of heat exchangers that utilize its cooling power to cool down and maintain the power components at the required operating temperatures.

3.1. Heat Exchangers

The power components in the aircraft's power architecture that require cooling are HTS generator, HTS motor, DC cables, power converters / invertors and fuel cell. Each power component operates at a different temperature range with different efficiency [14]. This efficiency and the operating temperature range are listed in Table 2. To achieve efficient heat exchange between H₂ fuel and the power components, we consider the simplest type of heat exchanger i.e., the pipe-in- pipe counter flow heat exchanger as shown in Figure 7. The hydrogen flowing in the inner pipe cools the gaseous helium flowing in the outer annulus. The cold GHe then cools the power component and maintains it under the required operating conditions. As liquid hydrogen flows through the heat exchangers it undergoes phase change to gaseous hydrogen initially and then its temperature rises as it approaches the fuel cell. Along the hydrogen flow path there will be a pressure drop. The pressure drop in the first heat exchanger that meets the cooling load of HTS generator is given by Equation 5.

$$\Delta P_{2\phi}^i = f_{LH_2} \frac{\dot{m}^2 L_i}{2\rho_{LH_2} A_i^2 D_i} \frac{1}{x_e - x_i} \int_{x_i}^{x_e} \phi_i^2(x) dx \quad (5)$$

where \dot{m} is hydrogen mass flow rate, which is a function of flight time, x_i and x_e is the inlet and exit quality fraction of Hydrogen as it undergoes phase change through the heat exchanger, ρ_{LH_2} is the

hydrogen density, f_{LH_2} is the friction factor corresponding to the Reynolds Number of the hydrogen flowing through the inner pipe of diameter D_i .

The tank pressure P_{tank} must be such that it equals the pressure drop in the heat exchangers in addition to the required fuel cell operating pressure as $P_{tank}(t) = \Delta P(t) + P_{fuel\ cell}$. Since, $P_{tank}(t)$ can only be tuned within a maximum value of 1.74 bar and minimum value of 1.3 bar, the heat exchanger design must be such that the pressure drop is within 0.44 bar. Assuming an inner pipe diameter, we calculate the length of the heat exchanger required to exchange the required cooling power. This gives a pressure drop in that heat exchanger. Similarly, it is followed for other heat exchangers. If the total pressure drop along the entire hydrogen flow path exceeds 0.44 bar, we tune the inner pipe diameter. The design and optimization of the heat exchangers could not be presented in detail here due to the page limitation. It will be presented in detail in our upcoming journal paper. A partial summary of the results is shown in Table 2. The maximum total pressure drop ΔP corresponding to the maximum mass flow rate is well within the tuning range.

Table 2. Heat Exchanger Summary

Equipment	Efficiency	Operating Temperature	Heat Load (kW)	HX Inner D (in)	HX Outer D (in)	HX Length (m)	HX Frictional loss (kPa) + Turn Loss (kPa)
Generator	99.96 %	30 K- 50 K	7.6	1.5	1.8	2.91	1.02
Motor	99.96 %	40 K- 60 K	7.6	1.5	1.8	1.80	1.20
DC Cable	250 W (per cable)	60 K- 70 K	1.5	1.5	1.8	0.30	0.30
Power Convertor	99 %	225K- 275K	380	3.0	4.8	3.40	0.3
Power Convertor				3.0	4.8	7.20	5.38 + 0.8
Fuel Cell	50 %	350 K	375.75	3.0	-	5.24	10.1 + 1.1
Fuel Cell			420.36	4.0	-	13.50	12 + 6
Total						34.35	38.2

3.2. Tank Pressure

The tank pressure P_{tank} required to achieve the desired LH₂ mass flow rate profile is shown in Figure 8.

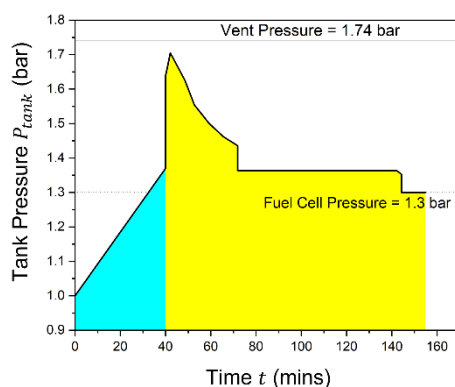


Figure 8. The tank pressure P_{tank} required to maintain the corresponding mass flow rate from the tank. During the flight waiting of 40 minutes the tank pressure rises following the closed tank system.

3.3. Flow Control

In our current design, the external heat in-leak is at 3.6 kW. This heat leak is large enough to avoid using the controlled boiling mechanism installed inside the storage tank. The required hydrogen mass flow rate can be maintained by the vapor flow rate control determined using Equation (6).

$$\dot{m}_{GH_2}(t)h_v = \dot{Q}_{leak}(t) - \dot{E}_{tank}(P_{tank}, t) - \dot{m}_{LH_2}(t)h_l \quad (6)$$

The resulting vapor flow rate control is shown in Figure 9. The controlled boiling mechanism is nonetheless installed just in case of emergency where a high-power consumption requirement arises.

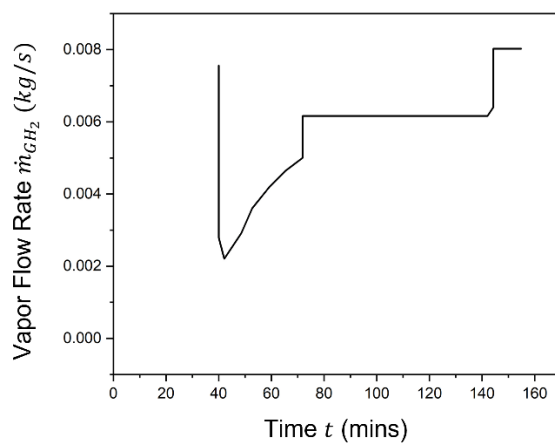


Figure 9. The required vapor flow control from the tank that needs to be maintained to execute the flight mission profile.

4. Summary

This work shows the LH₂ tank design and optimization to achieve a storage density of above 0.6. It is possible to achieve the desired fuel mass flow rate by regulating the tank pressure. The LH₂ cooling power is effectively utilized in meeting the cooling requirements of the aircraft's power architecture before its consumption in the fuel cell / generator.

5. References

- [1] Winnefeld, C., Kadyk, T., Bensmann, B., Krewer, U. and Hanke-Rauschenbach, R., 2018. Modelling and designing cryogenic hydrogen tanks for future aircraft applications. *Energies*, **11**(1), p.105.
- [2] Bills, A., Sripad, S., Fredericks, W.L., Singh, M. and Viswanathan, V., 2020. Performance metrics required of next-generation batteries to electrify commercial aircraft. *ACS Energy Letters*, **5**(2), pp.663-668.
- [3] Brewer, G.D. (1991). *Hydrogen Aircraft Technology* (1st ed.). Routledge. <https://doi.org/10.1201/9780203751480>
- [4] Timmerhaus, K.D. and Flynn, T.M., 2013. *Cryogenic process engineering*. Springer Science & Business Media.
- [5] Mills, G.L., Buchholtz, B. and Olsen, A., 2012, June. Design, fabrication and testing of a liquid hydrogen fuel tank for a long duration aircraft. In AIP conference proceedings (Vol. 1434, No. 1, pp. 773-780). American Institute of Physics.

- [6] Qiu, Y., Yang, H., Tong, L. and Wang, L., 2021. Research progress of cryogenic materials for storage and transportation of liquid hydrogen. *Metals*, 11(7), p.1101.
- [7] Woodcraft, A.L., 2005. Predicting the thermal conductivity of aluminium alloys in the cryogenic to room temperature range. *Cryogenics*, **45(6)**, pp.421-431.
- [8] Zheng, J., Chen, L., Wang, J., Xi, X., Zhu, H., Zhou, Y. and Wang, J., 2019. Thermodynamic analysis and comparison of four insulation schemes for liquid hydrogen storage tank. *Energy Conversion and Management*, 186, pp.526-534.
- [9] Anthony, F.M., Colt, J.Z. and Helenbrook, R.G., 1981. *Development and validation of cryogenic foam insulation for LH2 subsonic transports* (No. REPT-8654-927001). NASA
- [10] Bejan, A., 2013. *Convection heat transfer*. John wiley & sons.
- [11] Climente-Alarcon, V., Baskys, A., Patel, A. and Glowacki, B.A., 2019, April. Analysis of an on-line superconducting cryofan motor for indirect cooling by LH2. In *IOP Conference Series: Materials Science and Engineering* (Vol. **502**, No. 1, p. 012050). IOP Publishing.
- [12] Barbir, F., Balasubramanian, B. and Neutzler, J., 1999, August. Optimal operating temperature and pressure of PEM fuel cell systems in automotive applications. In *Abstracts of papers of the American chemical society* (Vol. 218, pp. U637-U637). 1155 16TH ST, NW, WASHINGTON, DC 20036 USA: AMER CHEMICAL SOC.
- [13] [Baratron® Capacitance Manometers \(mks.com\)](https://www.mks.com)
- [14] Barnola, I., Freeman, D., Cheetham, P., Yang, S., Kim, C.H. and Pamidi, S., 2019, August. Exploring options for integrated cryogenic circulation loop of superconducting power devices on electric aircraft. In *2019 AIAA/IEEE Electric Aircraft Technologies Symposium (EATS)* (pp. 1-8). IEEE.

Acknowledgement

The authors would like to acknowledge the support from NASA under Grant 80NSSC22M0068. The research was conducted at the National High Magnetic Field Laboratory, which is supported by National Science Foundation Cooperative Agreement No. DMR-1644779 and the State of Florida.